Physics Letters B 795 (2019) 682–688

Contents lists available at ScienceDirect

Physics Letters B

www.elsevier.com/locate/physletb

Quasi-free neutron and proton knockout reactions from light nuclei in a wide neutron-to-proton asymmetry range

M. Holl [a,b,c,d,*], V. Panin [a,e], H. Alvarez-Pol [f], L. Atar [a], T. Aumann [a,b], S. Beceiro-Novo [f], J. Benlliure [f], C.A. Bertulani [g], J.M. Boillos [f], K. Boretzky [b], M. Caamaño [f], C. Caesar [a,b], E. Casarejos [h], W. Catford [i], J. Cederkall [j], L. Chulkov [k], D. Cortina-Gil [f], E. Cravo [l], I. Dillmann [b,m], P. Díaz Fernández [n,f], Z. Elekes [o], J. Enders [a], L.M. Fraile [p], D. Galaviz Redondo [q,r], R. Gernhäuser [s], P. Golubev [j], T. Heftrich [t], M. Heil [b], M. Heine [u], A. Heinz [n], A. Henriques [q], H.T. Johansson [n], B. Jonson [n], N. Kalantar-Nayestanaki [v], R. Kanungo [c,d], A. Kelic-Heil [b], T. Kröll [a], N. Kurz [b], C. Langer [t], T. Le Bleis [s], S. Lindberg [n], J. Machado [w], E. Nacher [x], M.A. Najafi [v], T. Nilsson [n], C. Nociforo [b], S. Paschalis [a,y], M. Petri [a,y], R. Reifarth [t], G. Ribeiro [x], C. Rigollet [v], D.M. Rossi [a,b], D. Savran [z], H. Scheit [a], H. Simon [b], O. Sorlin [aa], I. Syndikus [a], O. Tengblad [x], Y. Togano [e], M. Vandebrouck [aa], P. Velho [q], F. Wamers [a,b], H. Weick [b], C. Wheldon [ab], G.L. Wilson [i], J.S. Winfield [b], P. Woods [ac], M. Zhukov [n], K. Zuber [ad,o], for the R^{3}B Collaboration

[a] *Institut für Kernphysik, Technische Universität Darmstadt, 64289 Darmstadt, Germany*
[b] *GSI Helmholtzzentrum für Schwerionenforschung, 64291 Darmstadt, Germany*
[c] *Saint Mary's University, B3H 3C3 Halifax, Nova Scotia, Canada*
[d] *TRIUMF, V6T 2A3 Vancouver, British Columbia, Canada*
[e] *RIKEN, Nishina Center for Accelerator-Based Science, 2-1 Hirosawa, 351-0198 Wako, Saitama, Japan*
[f] *IGFAE, Instituto Galego de Física de Altas Enerxías, Universidade de Santiago de Compostela, 15782 Santiago de Compostela, Spain*
[g] *Texas A&M University-Commerce, 75428 Commerce, TX, United States of America*
[h] *Universidad de Vigo, 36310 Vigo, Spain*
[i] *University of Surrey, Surrey GU2 7XH, United Kingdom*
[j] *Department of Physics, Lund University, 22100 Lund, Sweden*
[k] *NRC Kurchatov Institute, pl. Akademika Kurchatova, Moscow 123182, Russia*
[l] *CFTC, Faculdade de Ciencias, University of Lisbon, 1749-016 Lisbon, Portugal*
[m] *Justus-Liebig-Universität Gießen, 35392 Gießen, Germany*
[n] *Institutionen för Fysik, Chalmers Tekniska Högskola, S-412 96 Göteborg, Sweden*
[o] *ATOMKI Debrecen, Bem tér 18/c, 4026 Debrecen, Hungary*
[p] *Grupo de Física Nuclear & IPARCOS, Universidad Complutense de Madrid, 28040 Madrid, Spain*
[q] *Laboratory for Instrumentation and Experimental Particle Physics, LIP, 1649-003 Lisbon, Portugal*
[r] *Physics Department of the Faculty of Sciences, University of Lisbon, 1749-016 Lisbon, Portugal*
[s] *Technische Universität München, 85748 Garching, Germany*
[t] *Goethe-Universität Frankfurt, 60438 Frankfurt am Main, Germany*
[u] *IPHC-CNRS/Université de Strasbourg, 67037 Strasbourg, France*
[v] *KVI-CART, University of Groningen, 9747 AA Groningen, Netherlands*
[w] *LIBPhys-UNL, FCT, Universidade Nova de Lisboa, 2829-516 Caparica, Portugal*
[x] *Instituto de Estructura de la Materia, CSIC, E-28006 Madrid, Spain*
[y] *Department of Physics, University of York, York YO10 5DD, United Kingdom*
[z] *ExtreMe Matter Institute, GSI Helmholtzzentrum für Schwerionenforschung, 64291 Darmstadt, Germany*
[aa] *GANIL, Boulevard Henri Becquerel, 14076 Caen, France*
[ab] *University of Birmingham, Birmingham B15 2TT, United Kingdom*
[ac] *University of Edinburgh, Edinburgh EH8 9YL, United Kingdom*
[ad] *Technische Universität Dresden, Institut für Kern- und Teilchenphysik, 01069 Dresden, Germany*

* Corresponding author.
E-mail address: mholl@ikp.tu-darmstadt.de (M. Holl).

https://doi.org/10.1016/j.physletb.2019.06.069

ARTICLE INFO

Article history:
Received 8 January 2019
Received in revised form 4 June 2019
Accepted 4 June 2019
Available online 9 July 2019
Editor: D.F. Geesaman

Keywords:
Quasi-free scattering
Inverse kinematics
Shell model
Spectroscopic factors

ABSTRACT

The quasi-free scattering reactions ^{11}C$(p,2p)$ and ^{10,11,12}C(p,pn) have been studied in inverse kinematics at beam energies of 300–400 MeV/u at the R^{3}B-LAND setup. The outgoing proton-proton and proton-neutron pairs were detected in coincidence with the reaction fragments in kinematically complete measurements. The efficiency to detect these pairs has been obtained from GEANT4 simulations which were tested using the ^{12}C$(p,2p)$ and ^{12}C(p,pn) reactions. Experimental cross sections and momentum distributions have been obtained and compared to DWIA calculations based on eikonal theory. The new results reported here are combined with previously published cross sections for quasi-free scattering from oxygen and nitrogen isotopes and together they enable a systematic study of the reduction of single-particle strength compared to predictions of the shell model over a wide neutron-to-proton asymmetry range. The combined reduction factors show a weak or no dependence on isospin asymmetry, in contrast to the strong dependency reported in nucleon-removal reactions induced by nuclear targets at lower energies. However, the reduction factors for $(p,2p)$ are found to be 'significantly smaller than for (p,pn) reactions for all investigated nuclei.

The nuclear shell model is in its simplest form an independent-particle model (IPM), assuming that the nucleons move freely in an average potential. Nucleon-nucleon (NN) pairing correlations smear out the Fermi surface and distribute the single-particle strength among states within a few MeV. As a consequence, states below the Fermi energy are not fully occupied (as in the IPM) while states above are partly filled. This fragmentation of the spectroscopic strength is reproduced by the shell model (SM) by taking into account a residual interaction among valence nucleons for a given configuration space. The distribution of the spectroscopic strength is usually quantified by the spectroscopic factor (SF) associated with specific single-particle configurations. Theoretically, the SF for nucleon removal is defined as the norm of the overlap between the many-body wave functions of initial (A) and final (A-1) states. Experimentally, the SF is defined as the ratio of the measured nucleon-removal cross section populating a specific state of the A-1 nucleus and the corresponding theoretical cross section evaluated using a normalized single-particle wave function. Although SFs are not observables in a strict sense [1], they are very useful to discuss the shell structure of the involved nuclei and to quantify deviations from the above sketched single-particle picture.

Although the distribution of spectroscopic strength among available configurations around the Fermi surface depends on the effective interaction used in the shell model calculations, the shell model SFs add up to the sum-rule value $2j+1$ (corresponding to a fully occupied shell as expected in the IPM), if integrated over several MeV in excitation energy. The reduction of the spectroscopic strength beyond this fragmentation, i.e., beyond the shell model, is a long-standing problem in nuclear physics and is the topic of our experimental investigation presented in this Letter. Usually, this reduction of single-particle strength is quantified by a reduction factor R_s, which is defined as the ratio of the experimental cross section to a theoretical one including above described fragmentation, e.g., by including theoretical SM SFs. In order to not depend on a specific shell-model interaction, one can reduce the discussion to closed shell nuclei, or, one selects cases where the experimental removal cross section can be summed over A-1 states collecting all single-particle fragments in the energy range covered by the shell model. In that case, the reduction factors referring to the IPM and SM will be the same without dependence on a specific SM effective interaction.

Several quasi-elastic nucleon-knockout experiments using electron and proton beams led to a well-founded conjecture about the universality of a reduction (R_s) to 60–70 % compared to the IPM or SM expectation [2]. Our current understanding is that about half of this reduction is caused by coupling to collective phonons (particle-vibration coupling) resulting in a strong fragmentation of single-particle strength over many hole states in the 10 MeV excitation-energy domain [3]. This effect is often referred to as long-range correlations [4]. Another 15–20% reduction is attributed to NN short-range correlations (SRC) induced by the tensor and repulsive character of the NN interaction at short distances, an effect which additionally reduces the occupation probability of the single-particle states [4,5] resulting in a further fragmentation of the single-particle strength towards even higher excitation energies.

During the past two decades, nucleon-removal reactions in inverse kinematics using radioactive-ion beams and light nuclear targets (usually ^{9}Be or ^{12}C) have been used as a tool for the study of single-particle properties of nuclei far away from stability. These reactions made it possible to test the reduction of the spectroscopic strength for nucleon removal from exotic nuclei [6–10], confirming the findings of $(e,e'p)$ and $(p,2p)$ experiments in direct kinematics, and additionally suggesting a strong dependency of R_s on the nuclear isospin asymmetry [9,10]. Compared to the systematics obtained with stable nuclei, a stronger reduction is found for the removal of deeply bound valence nucleons while less reduction is found for the removal of the weakly bound abundant nucleon species. This systematic effect could point towards a stronger fragmentation of the single-particle strength for the more deeply bound rare nucleon species and/or to an increased effect of short-range correlations for the more deeply bound rare nucleon species. Recent experimental results from JLAB [11] indeed suggest that SRC pairs are dominated by n-p pairs implying a relatively larger probability for the rare nucleon species to form SRC pairs. Although *ab-initio* calculations including partially long-range and short-range NN correlations can account to a large extend for the reduction of spectroscopic strength close to the Fermi energy compared to the SM, the strong dependency on the isospin asymmetry as deduced from the experimental cross sections cannot be reproduced [4,12,13].

The reason for this asymmetry dependency is far from being clarified and could as well be related to a not fully understood reaction mechanism of the nucleon-removal process with nuclear targets and beam energies around 100 MeV/u and below where most of the data have been taken. The asymmetry dependency of R_s has also been investigated based on an analysis of transfer cross sections in Refs. [14–16] where no strong dependency was found. However, it was pointed out in Ref. [17] that the uncertainties in the reaction theory do not allow for a firm conclusion.

Table 1
Parameters of the beams and targets. Area densities of the CH_2 and carbon targets are indicated by ρ_{CH_2} and ρ_C, respectively. The values for the beam kinetic energy E_b and velocity β_b are given at the centre of each target. The spread in beam energies is caused by the energy loss in the targets and detectors in the beam line. For the secondary beam, also the momentum acceptance of the FRS of ±1% contributes to the range.

Isotope	ρ_{CH_2} [g/cm^2]	E_{b,CH_2} [MeV/u]	β_{b,CH_2}	ρ_C [g/cm^2]	$E_{b,C}$ [MeV/u]	$\beta_{b,C}$
^{10}C	0.94	385.5±4.5	0.707(2)	1.84	381.9±6.2	0.705(3)
^{11}C	0.94	325.4±4.7	0.671(3)	1.84	320.8±6.3	0.668(5)
^{12}C	0.21	397.8±0.5	0.713(1)	0.37	397.3±0.5	0.713(1)

A common property for both nucleon-removal and transfer reactions is their strong surface localization due to absorption effects in the nuclear medium. The suitability of nucleon-removal reactions to deduce spectroscopic factors for deeply bound nucleons has been questioned, and it has been proposed that asymptotic normalization coefficients (ANC) are better suited for the comparison to experimental data [18]. To overcome this limitation, the complementary method of quasi-free proton and neutron scattering, $(p, 2p)$ and (p, pn), has been extended to be used in inverse-kinematics experiments and to probe exotic nuclei [19,20]. In this case, a (radioactive-)ion beam of several hundred MeV/u impinges on a hydrogen target. Because elementary nucleon-nucleon cross sections become small at these energies, the transparency of the nucleus is maximize though final-state interactions, such as rescattering and absorption are substantial and have to be taken into account carefully. This makes quasi-free scattering (QFS) reactions a more suitable probe for the study of both weakly- and strongly-bound nucleon states [21,22]. In recent experimental studies of $(p, 2p)$ on oxygen isotopes, no or only a week dependency of R_s on the proton-neutron asymmetry was found [13,23].

A commonly used approach for the description of quasi-free scattering is the distorted-wave impulse approximation (DWIA) [24,25]. This approximation assumes a single interaction between the incident and the knocked-out nucleon, and incorporates effects of final-state interactions by distorting the single-nucleon wave functions using a complex optical potential. Recently, DWIA was combined with eikonal theory, leading to a model description similar to the one employed for nucleon-removal reactions induced by nuclei [22]. At the same time, other theoretical descriptions based on the Faddeev/Alt-Grassberger-Sandhas (Faddeev/AGS) framework [26,27] and the continuum-discretized coupled-channels (CDCC) method [28,29] have been developed as well. The latter reaction theory has been applied in Ref. [29] to study the asymmetry dependency based on the $(p, 2p)$ and (p, pn) knockout data of Refs. [13,30] coming to the same conclusion as Ref. [13], which was based on the eikonal approach [22].

In this Letter, we report on the first experimental results for quasi-free neutron knockout from stable and neutron-deficient carbon isotopes ^{10,11,12}C, as well as for quasi-free proton knockout from ^{11}C. For the comparison with theoretical cross sections, the same eikonal DWIA reaction framework is used as in the previous publication on oxygen isotopes [13], which agrees well with the cross sections computed in the CDCC approach [29] mentioned above. In addition, recently published results on quasi-free neutron knockout from neutron-rich nitrogen and oxygen isotopes [30] are compared to the same eikonal DWIA. Combined, these results allow for a systematic study of the quenching of spectroscopic strength over a wide range of isospin asymmetry using the (p, pn) reaction.

The presented results were obtained from two experiments performed at the R^{3}B-LAND setup at the GSI Helmholtzzentrum für Schwerionenforschung in Darmstadt. In both cases, the beams were provided by the heavy-ion synchrotron SIS-18. For the first experiment, a primary ^{12}C beam of 400 MeV/u was delivered directly to the experimental setup. For the second experiment, a secondary beam containing ^{10,11}C was produced by fragmentation of a primary 490 MeV/u ^{40}Ar beam on a 4 g/cm^2 Be target, and selected using the fragment separator FRS [31]. The measurements were performed with the R^{3}B-LAND setup, which is designed to measure reactions with relativistic radioactive beams in complete kinematics, making use of the strong kinematic forward focussing of the reaction products. Detailed descriptions of the setup can be found in Refs. [20,30]. To obtain QFS cross sections on hydrogen, separate measurements with polyethylene (CH_2) and carbon targets were performed. The experimental data with the carbon target were used to subtract the contribution of the carbon-induced reactions in CH_2 target.

Table 1 shows the properties of the targets used together with the beam energies and velocities at the centre of each target. The spread in beam energies is caused by the energy loss in the targets and detectors in the beamline. In case of the secondary beam, also the momentum acceptance of the FRS of ±1% contributes to the given range.

The incoming beam was identified on an event-by-event basis in terms of charge and mass-to-charge ratio. The magnetic rigidity of the outgoing particles was obtained utilizing position information from two double-sided silicon strip detectors (DSSD) in front of the dipole magnet ALADIN [32] and two fibre detectors behind [33]. In combination with the time of flight measured by a ToF-wall consisting of 32 scintillating paddles arranged in two layers and each read out by PMT tubes on both sides, the path of the particles through the magnetic field was reconstructed enabling mass identification and momentum measurement. The DSSDs and the ToF-wall also provided the charge identification of the outgoing particles through energy-loss measurements. To select QFS events with a pair of energetic ($E \gtrsim 20$ MeV) nucleons in the final state, two high-energy events in the 4π NaI array Crystal Ball (CB) [34], which surrounded the target area, were required in addition. The angular distributions of these nucleon pairs were dominated by nearly coplanar back-to-back scattering, a signature of QFS as shown in Ref. [20].

The unreacted beam was used to normalize the cross sections. As the unreacted beam is selected in the same manner as the reaction fragments, and the acceptance of the setup is close to 100% for all isotopes, efficiency corrections due to the identification of the fragments can be neglected. The only necessary correction to the cross section is therefore to account for the efficiency of the CB to detect both nucleons originating from the QFS reaction.

The two nucleons participating in the QFS process are scattered to large angles and have at their average emission angle of 45° energies around 150 to 200 MeV. The detection of nucleons and γ rays can easily be distinguished due to the high energy deposit of the nucleons in the NaI crystals of CB. A signal with $E \gtrsim 20$ MeV was assigned to the detection of a nucleon. Adjacent crystals with non-zero energy signals were assumed to belong to the same event and their energies were summed forming a cluster. Single crystals without adjacent high-energy hit were attributed to γ rays. They do not contribute to the cluster multiplicity, which requires at least one high-energy signal. The cluster multiplicity thus reflects closely the number of detected particles. As an example, the clus-

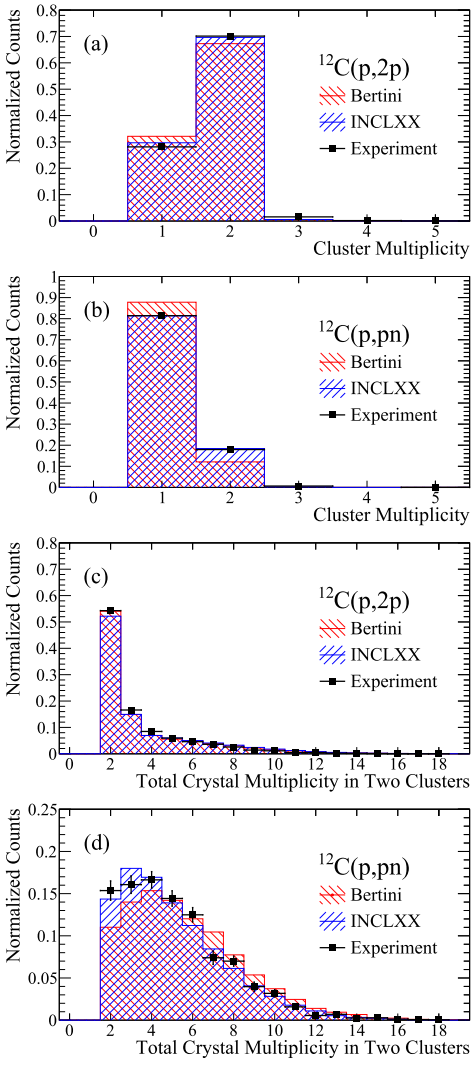

Fig. 1. Comparison of the experimental responses of the Crystal Ball NaI array (black circles with error bars) for ^{12}C$(p,2p)^{11}$B and ^{12}C$(p,pn)^{11}$C reactions with simulations using the R3BRoot framework with two different GEANT4 reaction models, the Bertini intranuclear cascade (red hatched) [35] and the Liège intranuclear cascade (INCLXX, blue hatched) [36]. Panels (a) and (b) show the number of high-energy clusters identified in $(p,2p)$ and (p,pn) reactions, respectively, with the condition to have at least one high-energy ($E \gtrsim 20$ MeV) event in the CB and a coincident final-state nucleus. Hits of crystals adjacent to a crystal with a high-energy entry are assumed to originate from the same particle and attributed to a cluster. The cluster multiplicity thus closely reflects the detected particle multiplicity. Panels (c) and (d) show the summed number of crystals constituting the clusters when exactly two clusters in one event are reconstructed, i.e., the total hit multiplicity when two particles have been identified.

ter multiplicities obtained in the ^{12}C$(p,2p)^{11}$B and ^{12}C$(p,pn)^{11}$C reactions are shown in the upper two frames in Fig. 1.

The detection efficiency ϵ to correctly identify both nucleons was determined from GEANT4 simulations using the R3BRoot framework [37] and the same analysis procedure as used to analyze the experimental data. A QFS reaction-kinematics code adapted from Ref. [38] and previously used in Ref. [20] was extended to simulate (p,pn) reactions. A realistic differential p-n cross section was introduced in the modified version of the code to account for the angular anisotropy of the p-n scattering in the centre-of-mass frame, adopting the parametrization of the free p-n cross section from the theoretical calculations in the PWA-framework outlined in Ref. [39]. In addition, two different GEANT4 reaction models based on the Bertini intranuclear cascade [35] and the Liège intranuclear cascade (INCLXX) [36] were tested in order to obtain the most reliable efficiency correction. For this purpose, simulated responses of the CB obtained with each model were compared to the experimental data for the ^{12}C$(p,2p)^{11}$B and ^{12}C$(p,pn)^{11}$C reactions. Fig. 1 shows the comparison of the simulated and experimentally obtained responses of the CB.

The experimental data is shown after subtraction of the carbon background. It is obvious from Figs. 1(a) and 1(b) that the INCLXX model gives a better agreement with the experimental data, and can correctly reproduce the observed cluster multiplicity distribution for both $(p,2p)$ and (p,pn) reactions. The difference in cluster multiplicity for $(p,2p)$ and (p,pn) events reflects the lower efficiency for neutron detection. The lower two panels display the total hit multiplicity for events with two clusters, i.e., when two particles are detected. The multiplicity distribution is much broader for (p,pn) reactions since the neutron detection requires a nuclear reaction in the crystal to produce light. Both models reproduce the distributions reasonably well, although a better description of the multiplicity for (p,pn) reactions with the INCLXX model can be recognized.

Since the cluster multiplicity is directly related to the efficiency, the very good reproduction of the experimental multiplicity data by the simulation based on the INCLXX model has been taken as evidence for a plausible description of the detection process by the simulation. All efficiencies used in the following have therefore been obtained with the INCLXX-based simulations. Uncertainties arising due to the statistics of the simulation and the slight change in kinematics for different final states are small. A systematic uncertainty due to the choice of thresholds in the addback procedure has been taken into account resulting in overall systematic uncertainties of the experimental cross sections of around 6 and 10% $(p,2p)$ and (p,pn) reactions, respectively.

The experimental cross sections $\sigma_{\rm exp}$ and reduction factors $R_s = \sigma_{\rm exp}/\sigma_{\rm th}$ obtained in this work are summarized in Table 2, together with cross sections recently reported in Refs. [13,20,30]. All theoretical cross sections were obtained with the eikonal-based DWIA reaction theory [22] and include shell-model SFs calculated with the OXBASH code using the WBT interaction [40] in the *spsdpf* model space restricted to $(0+1)\hbar\omega$. This explains the minor difference of R_s compared to Ref. [13], where the reduction factors refer to the IPM. However, the cases in Ref. [13] were chosen such, that the inclusive experimental cross sections are integrating effectively over the p-hole states in a wide enough energy window, or, exclusively contain the $p_{1/2}$ strength for those cases where all $p_{3/2}$ hole states are unbound. As mentioned earlier in the introduction, reduction factors referring to the IPM and the SM are very similar in that case. Indeed, the values given in Table 2 differ typically by only 1 to 5% compared to those referring to the IPM as given in Ref. [13], which does not affect our discussion. Although such a selection avoids to a large extent structure effects in the discussion of the reduction of single-particle strength, it reduces the number of nuclei available for a systematic study significantly, in particular for the extreme asymmetric cases or along an isotopic chain. For the systematic study presented here, we thus prefer to define the reduction factor relative to the SM, similar to previous studies on the systematics of one-nucleon removal reactions [10]. One should keep in mind, however, that R_s will then depend sensitively on the SM interaction used for the cases where the experimental cross section only contains a fraction of the single-particle strength close to the Fermi energy. This might induce a larger spread around a systematic behaviour of the reduction. For the neutron knockout ^{11}C(p,pn), for instance, the hole strength is distributed just around the particle threshold of ^{10}C ($S_p = 4.0$ MeV). The WBT shell-model interaction indeed distributes the spectroscopic strength partially ($\approx 60\%$, SF=1.86) below and partially above the threshold, while

Table 2
Measured and calculated cross sections and reduction factors are shown. The reaction is given in the first column. The values obtained in this work are listed together with the results from Refs. [13,20,30], see column 2. The difference in nucleon binding energy is given in the third column. The experimental cross sections are given in column 4, the used spectroscopic factors and theoretical cross sections in columns 5 and 6, and the reduction factors $R_s = \sigma_{exp}/\sigma_{th}$ in column 7. Parentheses following the values denote the statistical errors and systematical uncertainties, respectively.

Reaction	Ref.	ΔS [MeV]	σ_{exp} [mb]	$\sum C^2S$	σ_{th} [mb]	R_s
$^{11}C(p,2p)^{10}B$	this work	−4.4	18.2(9)(10)	2.66	21.3	0.86(4)(5)
$^{12}C(p,2p)^{11}B$	[20]	−2.7	19.2(18)(12)	4.28	32.0	0.60(6)(4)
$^{21}N(p,2p)^{20}C$	[30]	15.0	2.3(3)(1)	1.05	4.5	0.51(8)(1)
$^{14}O(p,2p)^{13}N$	[13]	−18.6	10.2(8)(7)	1.97	14.9	0.69(5)(5)
$^{16}O(p,2p)^{15}N$	[13]	−3.5	26.8(9)(17)	6.09	38.9	0.69(2)(4)
$^{17}O(p,2p)^{16}N$	[13]	9.6	7.9(3)(5)	2.07	12.6	0.63(2)(4)
$^{21}O(p,2p)^{20}N$	[13]	17.2	5.3(2)(3)	1.88	8.6	0.61(3)(4)
$^{22}O(p,2p)^{21}N$	[13,30]	16.4	5.9(4)(4)	2.60	11.1	0.53(4)(4)
$^{23}O(p,2p)^{22}N$	[13]	22.3	5.0(10)(3)	1.98	8.0	0.62(12)(4)
$^{10}C(p,pn)^{9}C$	this work	17.3	16.3(22)(14)	1.74	16.4	0.99(13)(9)
$^{11}C(p,pn)^{10}C$	this work	4.4	17.0(15)(21)	1.86	16.0	1.06(9)(12)
$^{12}C(p,pn)^{11}C$	this work	2.7	30.0(32)(27)	4.28	37.3	0.80(9)(7)
$^{21}N(p,pn)^{20}N$	[30]	−15.0	48.5(39)(10)	5.60	55.4	0.88(7)(2)
$^{22}O(p,pn)^{21}O$	[30]	−16.4	39.2(22)(8)	5.98	48.6	0.81(5)(2)
$^{23}O(p,pn)^{22}O$	[30]	−22.3	54 (11)(1)	8.05	70.5	0.77(15)(2)

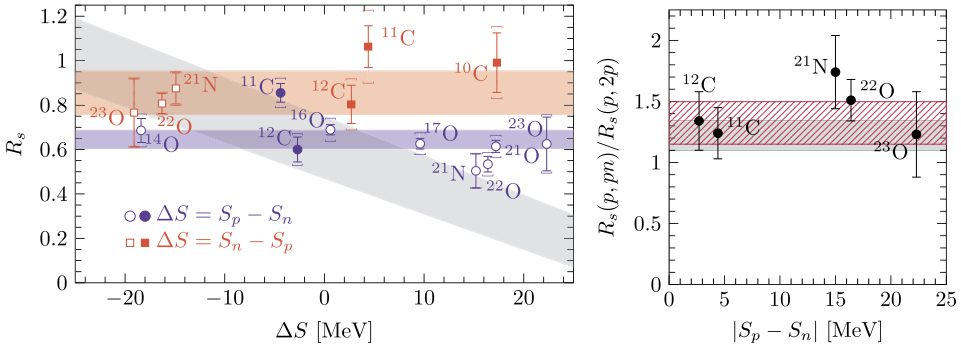

Fig. 2. Left: the reduction factor $R_s = \sigma_{exp}/\sigma_{th}$ as a function of the difference in nucleon binding energy ΔS. Blue circles denote the results from $(p,2p)$, red squares from (p,pn). The error bars represent the statistical uncertainty, the square brackets the total uncertainty including systematical errors. The dependency found in nucleon-removal reactions with nuclear targets [10] is indicated by the grey shaded area. The horizontal bands indicate the average reduction factor for each type of reaction. Right: The ratios of reduction factors for (p,pn) and $(p,2p)$ as a function of the difference in binding energy. The purple-hatched band indicates the ratio of the average reduction factors, the grey band the ratios of spectroscopic factors observed in direct kinematics [41].

only population of bound states contributes to the $A(p,pN)A-1$ cross section.

The systematics of obtained reduction factors R_s is shown in Fig. 2 (left) as a function of the difference in nucleon binding energy ΔS, which reflects the difference in their Fermi energies and is a measure for the neutron-to-proton asymmetry. If only one final state contributes to the cross section, $\Delta S = S_n - S_p$ for neutron removal and $\Delta S = S_p - S_n$ for proton removal, where $S_{n,p}$ are the nucleon separation energies with respect to the final state. In case several final states contribute, ΔS represents the weighted average. Large positive (negative) values of ΔS correspond thus to the removal of a strongly (weakly) bound nucleon of the rare (abundant) species from a very asymmetric nucleus.

The R_s values are displayed as blue circles (red squares) for proton (neutron) removal reactions. Values shown as filled symbols are based on the cross sections from this work, while values for R_s based on previously published cross sections are given as open symbols. The systematic trend of R_s with asymmetry obtained from the analysis of a large number of nucleon-removal reactions induced by nuclear targets [10] is indicated by the grey-shaded area. The quasi-free $(p,2p)$ and (p,pn) knockout data do not exhibit this trend but scatter around an average value indicated by the two horizontal coloured bands for proton (blue) and neutron (red) removal. However, the average reduction factors are found to be smaller for $(p,2p)$ than for (p,pn) with $R_s = 0.65(4)$ and $R_s = 0.85(10)$, respectively, showing a relative difference of 32(6)% between the two reactions. This is also shown in Fig. 2 (right) where the ratio of the reduction factors is shown as a function of $|\Delta S|$ for the nuclei for which both reactions were measured. The ratio of the average reduction factors is indicated by the purple hatched band. The difference is similar to measurements in direct kinematics, shown by the grey band, in which spectroscopic factors extracted from (p,pn) were found to be 15–25% larger than those extracted from $(p,2p)$[41].

Taking into account the isospin symmetry of ^{12}C, a surprisingly small reduction of spectroscopic strength ($R_s = 0.80(11)$, corresponding to a spectroscopic factor $S = 3.44(36)$) is found in $^{12}C(p,pn)^{11}C$ reactions as compared to the $(p,2p)$ case, for which $R_s = 0.60(7)$ is consistent with previous $(e,e'p)$ and $(p,2p)$ measurements in direct kinematics. Similar results were reported recently for the direct-kinematics measurement of the $^{12}C(p,pn)^{11}C$ reaction using a 296-MeV polarized proton beam, where the spectroscopic factor $S = 3.94 \pm 0.09 \pm 1.02$ was extracted [42] using another well-established theoretical DWIA model [25]. The analysis in Ref. [41] reports a value of 1.15 for ^{12}C and 1.24 ± 0.13 and 1.20 ± 0.12 for ^{16}O for removal from the $p_{1/2}$ and $p_{3/2}$ orbits, respectively. The reason for this systematic difference in proton- and neutron-removal reactions is not clear. Future experimental and theoretical investigations have to clarify if this is related to deficiencies in the reaction model. At the moment, we can only

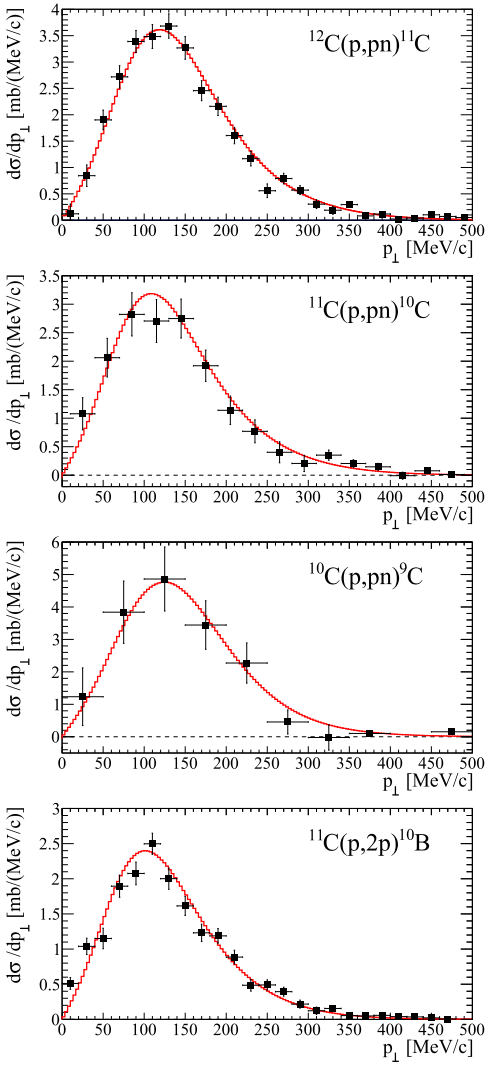

Fig. 3. Comparison of the measured transverse momentum distributions (points) to the eikonal theory calculations following the model described in Ref. [22], assuming the removal of a nucleon from the p-shell (curves). There is good agreement between data and calculations in all four cases.

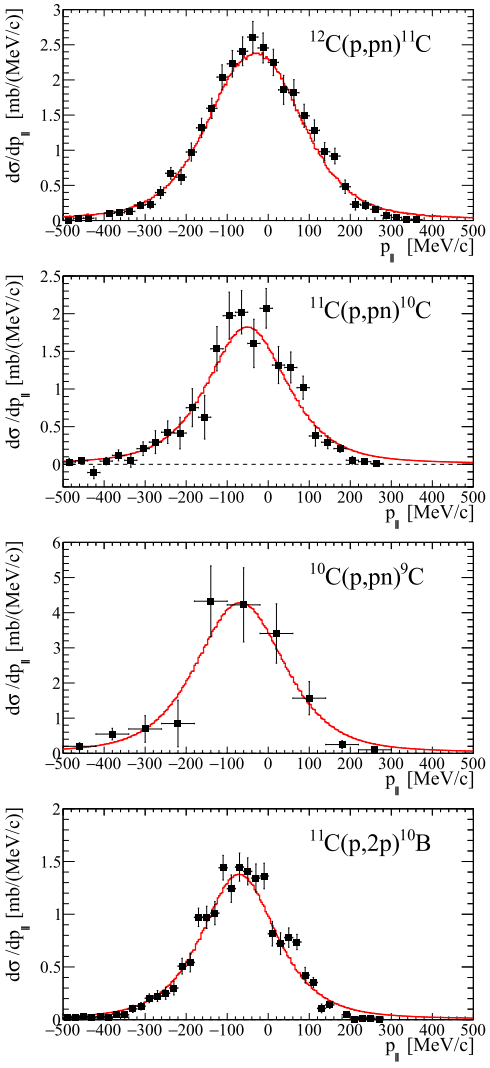

Fig. 4. Comparison of the measured parallel momentum distributions (points) to the eikonal theory calculations following the model described in Ref. [22] and assuming the removal of a nucleon from the p-shell (curves). The calculated distributions have been shifted to match the centroid of the experimental distributions.

speculate. An apparent difference between $(p, 2p)$ and (p, pn) reactions is the sizeable difference of the pp and np cross sections and in particular its different energy dependence in the energy range discussed here. Experiments at different beam energies covering the range from the minimum to the maximum of the NN cross section, i.e., from 300 to 800 MeV, would be very valuable to test the reaction theory.

The measured transverse momentum distributions of the outgoing residual nuclei from the QFS reactions are shown in Fig. 3. They are compared to the theoretical momentum distributions following the model described in Ref. [22], which assumes quasi-free knockout of a particle from the p-shell. The calculated distributions have been convoluted with the experimental response, i.e., the momentum profile of the unreacted beam, and scaled to the experimental cross sections. Since the theoretical distribution is derived using a normalized single-particle wave function, the scaling factor corresponds to the spectroscopic factor. The shape of the experimental and calculated distributions agree well for all four reactions. In a similar way, Fig. 4 shows the measured and calculated parallel momentum distributions which are Lorentz-transformed into the rest-frame of the parent nucleus. The experimental parallel momentum distributions appear to be slightly shifted towards negative values reflecting momentum and energy conservation in the QFS reaction. This shift is not considered in the eikonal model due to the approximation that the beam energy is much larger than the separation energy (energy conservation is neglected here) leading to symmetric distributions centred at zero. In this case the calculated distributions have not only been scaled and convoluted with the experimental resolution but also shifted by 30–80 MeV/c to match the position of the experimental maximum. The asymmetry in the parallel momentum distribution has been discussed in detail in the recent theoretical work of Ogata et al. [43]. Despite the fact that the momentum shift cannot be reproduced by the eikonal model used in the present work, the results of Ref. [43] indicate that the shift has a quite small effect ($\sim 5\%$) on the integrated QFS cross sections, especially for energies above 200 MeV/u. In contrast to reactions at lower beam energies, the experimental distributions are almost symmetric reflecting the fact that the beam energy is high enough to fulfil the approximations made in the eikonal theory (see, e.g., the discussion on asymmetric momentum distributions in Ref. [43]).

In summary, we have investigated QFS reactions in inverse kinematics using unstable and stable carbon isotopes. Integral (p, pn) and $(p, 2p)$ cross sections for the ^{10,11,12}C nuclei on a hydrogen target have been extracted for the first time deploying the large acceptance and complete-kinematics capabilities of the R^{3}B-LAND setup. Experimental recoil momentum distributions of the residual fragments can be well described by the eikonal reaction theory assuming removal from $l = 1$ single-particle states in the nuclei of interest. The experimental cross sections are used to determine the spectroscopic strength for the valence p-shell nucleons in ^{10}C, ^{11}C and ^{12}C. In addition, previously published cross sections for nucleon-removal from nitrogen and oxygen isotopes have been analyzed in the same way providing a systematic study of the reduction R_s of the spectroscopic strength as a function of neutron-proton asymmetry in a wide range. The deduced reduction R_s does not show the well-pronounced isospin-asymmetry dependency reported in nucleon-removal reactions with nuclear targets. This is in agreement with recently reported analyzes of $(p, 2p)$ knockout reactions on the oxygen chain and a number of recent theoretical studies.

However, a discrepancy is found to exist between the reduction factors for proton and neutron removal for all investigated nuclei, including the symmetric ^{12}C nucleus, which is consistent with a recent analysis of QFS measurements in direct kinematics [41]. The reason for this discrepancy is not clear but can be most likely attributed to the uncertainties in the applied reaction models. If so, then this effect might alter also the isospin dependency of calculated cross sections. A final conclusion on the asymmetry dependency should thus be drawn only after having understood the difference between $(p, 2p)$ and (p, pn) reactions. Further theoretical and experimental investigations using $(p, 2p)$ and (p, pn) reactions both in direct and inverse kinematics and at different beam energies are required to resolve this puzzle.

Acknowledgements

This work was supported by the German Federal Ministry of Education and Research (BMBF projects 05P2015RDFN1 and 05P15WOFNA), through the GSI-TU Darmstadt cooperation agreement, by the State of Hesse through the LOEWE center HIC for FAIR, and the Helmholtz-Gemeinschaft through the graduate school HGS-HIRe. This work was supported by the European Union by means of the European Commission within its Seventh Framework Program (FP7) via ENSAR (Contract No. 262010), and the Spanish CICYT research grants FPA2012-32443, FPA2015-64969-07387, and FPA2015-69640-C2-1-P. This work has supported by the Swedish Research Council under contract number 621-2011-5324. C.A.B. acknowledges support from the U.S. NSF grant No. 1415656 and the U.S. DOE grant No. DE-FG02-08ER41533. Supported by the Portuguese FCT under the project PTDC/FIS/103902/2008.

References

[1] R. Furnstahl, H.-W. Hammer, Phys. Lett. B 531 (2002) 203, https://doi.org/10.1016/S0370-2693(01)01504-0.
[2] G.J. Kramer, H.P. Blok, L. Lapikás, Nucl. Phys. A 679 (2001) 267, https://doi.org/10.1016/S0375-9474(00)00379-1.
[3] C. Mahaux, P. Bortignon, R. Broglia, C. Dasso, Phys. Rep. 120 (1985) 1, https://doi.org/10.1016/0370-1573(85)90100-0.
[4] W.H. Dickhoff, C. Barbieri, Prog. Part. Nucl. Phys. 52 (2004) 377, https://doi.org/10.1016/j.ppnp.2004.02.038.
[5] O. Hen, et al., Rev. Mod. Phys. 89 (2017) 045002, https://doi.org/10.1103/RevModPhys.89.045002.
[6] B.A. Brown, et al., Phys. Rev. C 65 (2002) 061601, https://doi.org/10.1103/PhysRevC.65.061601.
[7] P.G. Hansen, J.A. Tostevin, Annu. Rev. Nucl. Part. Sci. 53 (2003) 219, https://doi.org/10.1146/annurev.nucl.53.041002.110406.
[8] J. Enders, et al., Phys. Rev. C 67 (2003) 064301, https://doi.org/10.1103/PhysRevC.67.064301.
[9] A. Gade, et al., Phys. Rev. C 77 (2008) 044306, https://doi.org/10.1103/PhysRevC.77.044306.
[10] J.A. Tostevin, A. Gade, Phys. Rev. C 90 (2014) 057602, https://doi.org/10.1103/PhysRevC.90.057602.
[11] M. Duer, et al., Nature 560 (2018) 617, https://doi.org/10.1038/s41586-018-0400-z.
[12] G.F. Grinyer, et al., Phys. Rev. Lett. 106 (2011) 162502, https://doi.org/10.1103/PhysRevLett.106.162502.
[13] L. Atar, et al., Phys. Rev. Lett. 120 (2018) 052501, https://doi.org/10.1103/PhysRevLett.120.052501.
[14] J. Lee, et al., Phys. Rev. C 83 (2011) 014606, https://doi.org/10.1103/PhysRevC.83.014606.
[15] F. Flavigny, et al., Phys. Rev. Lett. 110 (2013) 122503, https://doi.org/10.1103/PhysRevLett.110.122503.
[16] F. Flavigny, N. Keeley, A. Gillibert, A. Obertelli, Phys. Rev. C 97 (2018) 034601, https://doi.org/10.1103/PhysRevC.97.034601.
[17] F. Nunes, A. Deltuva, J. Hong, Phys. Rev. C 83 (2011) 034610, https://doi.org/10.1103/PhysRevC.83.034610.
[18] A.M. Mukhamedzhanov, A.S. Kadyrov, Phys. Rev. C 82 (2010) 051601, https://doi.org/10.1103/PhysRevC.82.051601.
[19] T. Kobayashi, et al., Nucl. Phys. A 805 (2008) 431, https://doi.org/10.1016/j.nuclphysa.2008.02.282.
[20] V. Panin, et al., Phys. Lett. B 753 (2016) 204, https://doi.org/10.1016/j.physletb.2015.11.082.
[21] G. Jacob, T.A.J. Maris, Rev. Mod. Phys. 45 (1973) 6, https://doi.org/10.1103/RevModPhys.45.6.
[22] T. Aumann, C.A. Bertulani, J. Ryckebusch, Phys. Rev. C 88 (2013) 064610, https://doi.org/10.1103/PhysRevC.88.064610.
[23] S. Kawase, et al., Prog. Theor. Exp. Phys. 2018 (2) (2018) 021D01, https://doi.org/10.1093/ptep/pty011.
[24] N.S. Chant, P.G. Roos, Phys. Rev. C 15 (1977) 57, https://doi.org/10.1103/PhysRevC.15.57.
[25] N.S. Chant, P.G. Roos, Phys. Rev. C 27 (1983) 1060, https://doi.org/10.1103/PhysRevC.27.1060.
[26] R. Crespo, A. Deltuva, E. Cravo, Phys. Rev. C 90 (2014) 044606, https://doi.org/10.1103/PhysRevC.90.044606.
[27] E. Cravo, R. Crespo, A. Deltuva, Phys. Rev. C 93 (2016) 054612, https://doi.org/10.1103/PhysRevC.93.054612.
[28] A.M. Moro, Phys. Rev. C 92 (2015) 044605, https://doi.org/10.1103/PhysRevC.92.044605.
[29] M. Gómez-Ramos, A.M. Moro, Phys. Lett. B 785 (2018) 511, https://doi.org/10.1016/j.physletb.2018.08.058.
[30] P. Díaz Fernández, et al., Phys. Rev. C 97 (2018) 024311, https://doi.org/10.1103/PhysRevC.97.024311.
[31] H. Geissel, et al., Nucl. Instrum. Methods B 70 (1992) 286, https://doi.org/10.1016/0168-583X(92)95944-M.
[32] J. Hubele, et al., Z. Phys. A 340 (3) (1991) 263–270, https://doi.org/10.1007/BF01294674.
[33] K. Mahata, et al., Nucl. Instrum. Methods A 608 (2) (2009) 331–335, https://doi.org/10.1016/j.nima.2009.07.012.
[34] V. Metag, et al., Nucl. Phys. A 409 (1983) 331–342, https://doi.org/10.1016/0375-9474(83)90695-4.
[35] D.H. Wright, M.H. Kelsey, et al., Nucl. Instrum. Methods A 804 (2015) 175, https://doi.org/10.1016/j.nima.2015.09.058.
[36] A. Boudard, et al., Phys. Rev. C 87 (2013) 014606, https://doi.org/10.1103/PhysRevC.87.014606, arXiv:1210.3498.
[37] D. Bertini, J. Phys. Conf. Ser. 331 (2011) 032036, https://doi.org/10.1088/1742-6596/331/3/032036.
[38] L.V. Chulkov, et al., Nucl. Phys. A 759 (2005) 43, https://doi.org/10.1016/j.nuclphysa.2005.05.148.
[39] V.G.J. Stoks, et al., Phys. Rev. C 48 (1993) 792, https://doi.org/10.1103/PhysRevC.48.792.
[40] E.K. Warburton, B.A. Brown, Phys. Rev. C 46 (1992) 923, https://doi.org/10.1103/PhysRevC.46.923.
[41] T. Wakasa, K. Ogata, T. Noro, Prog. Part. Nucl. Phys. 96 (2017) 32, https://doi.org/10.1016/j.ppnp.2017.06.002.
[42] T. Wakasa, et al., Phys. Rev. C 96 (2017) 014604, https://doi.org/10.1103/PhysRevC.96.014604.
[43] K. Ogata, K. Yoshida, K. Minomo, Phys. Rev. C 92 (2015) 034616, https://doi.org/10.1103/PhysRevC.92.034616.